

# Intramolecular Catalysis of Amide Isomerization: Kinetic Consequences of the 5-NH- $N_a$ Hydrogen Bond in Prolyl Peptides

Christopher Cox and Thomas Lectka\*

Contribution from the Department of Chemistry, Johns Hopkins University, Baltimore, Maryland, 21218

Received May 1, 1998

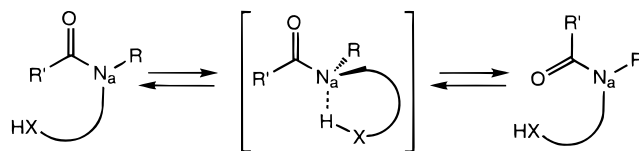
**Abstract:** The presence of an intramolecular hydrogen bond has been proposed to play a key role in the catalysis of amide isomerization by peptidylprolyl isomerases (PPIases), which are highly conserved and ubiquitous rotamase enzymes that catalyze the *cis*–*trans* isomerization of proline residues in peptides and proteins. We present herein kinetic and spectroscopic evidence that indicates the existence of an intramolecular hydrogen bond between the prolyl amide nitrogen and the adjacent amidic NH within a five-membered ring (the 5-NH- $N_a$  hydrogen bond) that is capable of catalyzing proline isomerization by up to 260-fold in model prolyl peptides. Our results provide the first systematic study of intramolecular general-acid-catalyzed amide isomerization.

## Introduction

The catalysis of amide isomerization by strong Brønsted acids is a well-known process that proceeds through a putative N-protonated intermediate present in low concentration.<sup>1</sup> The carbonyl oxygen of amides is universally believed to be the preferred site of protonation in aqueous acidic media;<sup>2</sup> however, acid-catalyzed amide isomerization must proceed through the disfavored N-protonated intermediate wherein we expect nearly free rotation about the C–N bond due to complete loss of conjugation between the nitrogen lone pair and the carbonyl  $\pi$ -cloud.<sup>3</sup> Only a very small percentage of amide molecules need be N-protonated to effect a sizable overall barrier lowering,<sup>2b,4</sup> but this nevertheless requires exposure of the amide to a solution of low pH. For example, the rate of amide isomerization in DMA (dimethylacetamide) increases 130-fold when the pH of the solution is lowered from 7.0 to 1.8.<sup>1b</sup> Given the importance of the amide functional group in biological systems, the question of whether N-protonation of amides plays a role in biological processes, such as the catalysis of protein folding, becomes a significant one.

Nature, rather than operate with strong Brønsted acidic media, tends to avoid harsh, low-pH conditions by rendering processes intramolecular, thereby gaining effective molarity through pinpointed spatial proximity. Intramolecular general acid-catalyzed amide isomerization of this type is pictured in Scheme 1 as a process in which hydrogen bond (H-bond)<sup>5</sup> or proton

**Scheme 1.** Intramolecular Catalysis of Amide Isomerization



donation to the amide nitrogen ( $N_a$ ) through a correctly aligned cyclic intermediate replaces discrete intermolecular N-protonation. Karplus has reported theoretical results that implicate this interaction as a mechanism in the catalysis of *cis*–*trans* proline isomerization by rotamase enzymes,<sup>6</sup> and we have presented the first experimental support of this interaction in a recent Communication.<sup>7</sup>

The *cis*–*trans* isomerization of prolyl peptide bonds is an inherently slow process with a free energy of activation ( $\Delta G^\ddagger$ ) of 20–22 kcal/mol in aqueous solution, and is known to be the slow step in the folding of many proline-containing proteins.<sup>8</sup> FKBP and cyclophilin are rotamase enzymes, or peptidylprolyl isomerases (PPIases), that catalyze this isomerization, both for model peptides and proteins *in vitro*<sup>1a,8a</sup> as well as *in vivo*.<sup>9</sup> The PPIases<sup>10</sup> have also been found to be the cellular targets of immunosuppressive drugs used to prevent graft rejection in humans;<sup>11</sup> however, there appears to be no direct relationship between the immunosuppressive function and isomerase activity.<sup>12</sup> Although the full extent of the biological roles played

(1) (a) Stein, R. L. *Adv. Protein Chem.* **1993**, *44*, 1. (b) Gerig, J. T. *Biopolymers* **1971**, *10*, 2435. (c) Steinberg, I. Z.; Harrington, W. F.; Berger, A.; Sela, M.; Katchalski, E. *J. Am. Chem. Soc.* **1960**, *82*, 5263. Perrin investigated the mechanism of acid-catalyzed proton exchange in amides; see: (d) Perrin, C. L. *Acc. Chem. Res.* **1989**, *22*, 268.

(2) (a) Homer, R. B.; Johnson, C. D. In *The Chemistry of Amides*; Zabicky, J., Ed.; Wiley: New York, 1970; Chapter 3. (b) The  $pK_a$  of an O-protonated amide is close to zero, whereas an N-protonated amide has a  $pK_a$  of about –7; see: Williams, A. *J. Am. Chem. Soc.* **1976**, *98*, 5645.

(3) On the other hand, hydrogen bonding to the carbonyl oxygen or O-protonation will have a barrier-raising effect on amide isomerization; see: (a) Scheiner, S.; Kern, C. W. *J. Am. Chem. Soc.* **1977**, *99*, 7042. (b) Neuman, R. C., Jr.; Woolfenden, W. R.; Jonas, V. *J. Phys. Chem.* **1969**, *73*, 3177.

(4) (a) Martin, R. B.; Hutton, W. C. *J. Am. Chem. Soc.* **1973**, *95*, 4752. (b) Martin, R. B. *J. Chem. Soc., Chem. Commun.* **1972**, 793.

(5) List of abbreviations: IC, intramolecular catalysis;  $N_a$ , prolyl amide nitrogen; H-bond, hydrogen bond; ST, saturation transfer NMR; DHFR, dihydrofolate reductase; FKBP, binding protein for the immunosuppressive agent FK-506; PPIase, peptidylprolyl isomerase (generic term for cyclophilin and/or FKBP); EDCI, 1-(3-dimethylaminopropyl)-3-ethylcarbodiimide hydrochloride, a water soluble carbodiimide used in peptide coupling.

(6) (a) Fischer, S.; Dunbrack, R. L., Jr.; Karplus, M. *J. Am. Chem. Soc.* **1994**, *116*, 11931. (b) Fischer, S.; Michnick, S.; Karplus, M. *Biochemistry* **1993**, *32*, 13830.

(7) Cox, C.; Young, V. G., Jr.; Lectka, T. *J. Am. Chem. Soc.* **1997**, *119*, 2307.

(8) (a) Schmid, F. X.; Mayr, L. M.; Mücke, M.; Schönbrunner, E. R. *Adv. Protein Chem.* **1993**, *44*, 25. (b) Schmid, F. X. In *Protein Folding*; Creighton, T. E., Ed.; Freeman: New York, 1992; Chapter 5. (c) Fisher, G.; Schmid, F. X. *Biochemistry* **1990**, *29*, 2205. (d) Brandts, J. F.; Halvorson, H. R.; Brennan, M. *Biochemistry* **1975**, *14*, 4953.

by these novel enzymes has yet to be established, their importance is supported by the observation that they are ubiquitous and highly conserved in organisms ranging from *E. coli* to humans.<sup>11</sup>

The detailed mechanisms by which the PPIases catalyze *cis*–*trans* isomerization remain to be completely elucidated. Thorough knowledge of these mechanisms is required to design better inhibitors for studies of the immunosuppressive and protein folding roles of the PPIases, and also to examine other postulated roles of these enzymes *in vivo*.<sup>13</sup> One important aspect of the PPIase mechanism that has been proposed based on theoretical studies is intramolecular catalysis, whereby the prolyl nitrogen becomes an H-bond acceptor in the rotational transition state for amide isomerization (Figure 1).<sup>6,14</sup> Intramolecular catalysis is also believed to play a key role in the nonenzymatic folding of some proteins including dihydrofolate reductase (DHFR, Figure 1B).<sup>15</sup> Substrates bound in the active site of FKBP are postulated to adopt a type VIa proline turn,<sup>6</sup> in which the amide proton of the residue that follows the proline in primary sequence sits directly above the ring and can donate an H-bond to the prolyl N<sub>a</sub> (Figure 1A, the 5-NH–N<sub>a</sub> H-bond); this stabilizing interaction has been calculated to contribute 1.4 of the 6.2 kcal/mol decrease in  $\Delta G^\ddagger$  for FKBP-catalyzed proline isomerization.<sup>6b</sup> On the other hand, cyclophilin binds its substrates in a type VIb proline turn, in which the adjacent amide

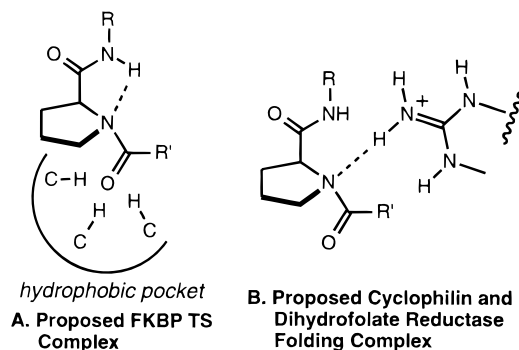


Figure 1. Intramolecular catalysis in biological systems.

proton is not properly aligned to induce intramolecular catalysis. However, by analogy to the proposed folding of DHFR,<sup>15</sup> there is an Arg residue close in tertiary structure within the active site of cyclophilin (but not in the active site of FKBP) that may act as the hydrogen bond donor during catalysis (Figure 1B).<sup>6b</sup>

Intramolecular hydrogen bonding between a prolyl N<sub>a</sub> and nearby H-bond donors is quite common in structural protein chemistry, yet its role in the folding and stabilization of proteins is often ignored.<sup>16</sup> Matthews examined H-bonding patterns in the crystal structures of 42 proteins determined at high resolution and found that eight have strong H-bond donors (Arg, His, Lys) within 4 Å of a prolyl nitrogen; 12 more H-bonds were identified in this same set of proteins if neutral donors were included.<sup>15</sup> Additionally, there are a sizable number of cyclic peptidic natural products which contain a 5-NH–N<sub>a</sub> H-bond, as evidenced by crystal structures,<sup>17</sup> as well as the spirocyclic peptidomimetics synthesized by Johnson.<sup>18</sup> It has yet to be established conclusively whether H-bonds to prolyl nitrogens are involved in intramolecular catalysis of protein folding, but these interactions clearly occur with considerable frequency in nature.

In a preliminary report, we provided the first experimental evidence for intramolecular catalysis in model systems (substituted prolines) attributed to the 5-NH–N<sub>a</sub> H-bond depicted in Figure 1A.<sup>7</sup> We now describe a comprehensive experimental study of this interaction in model systems, and have expanded its scope to include the following: (1) correlation between the Hammett  $\sigma_p$  values of remote substituents and the kinetics of observed intramolecular catalysis; (2) extensive spectroscopic characterization of the intramolecular 5-NH–N<sub>a</sub> H-bond; (3) intramolecular catalysis of prolyl carbamates in organic and aqueous/organic solution; (4) intramolecular catalysis observed in “polar” chlorocarbon solvents such as CH<sub>2</sub>Cl<sub>2</sub> or CHCl<sub>3</sub> is less than that possible in a very nonpolar, non-hydrogen bonding solvent such as CCl<sub>4</sub>; and (5) proof that intramolecular catalysis is due to an H-bond and not to discrete N-protonation of the prolyl N<sub>a</sub>.

(9) There have only been a few reports of PPIases acting as folding catalysts *in vivo*: (a) For the role of cyclophilin in the maturation of the collagen triple helix, see: Steinmann, B.; Bruckner, P.; Superti-Furga, A. *J. Biol. Chem.* **1991**, *266*, 1299. (b) For cyclophilin catalyzed folding of the monomeric protein transferrin, see: Lodish, H. F.; Kong, N. *J. Biol. Chem.* **1991**, *266*, 14835. (c) For the possible role of PPIases in protein biogenesis in a eukaryotic cytosol, see: Kruse, M.; Brunke, A. E.; Escher, A.; Szalay, A. A.; Tropschug, M.; Zimmermann, R. *J. Biol. Chem.* **1995**, *270*, 2588.

(10) The terminology used in the literature for rotamase enzymes can be ambiguous. “PPIase” was originally synonymous with cyclophilin, but the current usage, and the one we adopt here, is to use PPIase as a generic term encompassing both cyclophilin and FKBP. When we wish to refer to a specific enzyme, we will clearly differentiate between them.

(11) (a) Fruman, D. A.; Burakoff, S. J.; Bierer, B. E. *FASEB J.* **1994**, *8*, 391. (b) Belshaw, P. J.; Meyer, S. D.; Johnson, D. D.; Romo, D.; Ikeda, Y.; Andrus, M.; Alberg, D. G.; Schultz, L. W.; Clardy, J.; Schreiber, S. L. *Synlett.* **1994**, 381.

(12) It is known that the catalysis of *cis*–*trans* amide isomerization is not the direct function of the PPIases in immunosuppression; rather, a complex of the immunosuppressive drug and the enzyme is believed to bind to the protein phosphatase calcineurin, and thereby inhibit T-cell activation. The immunosuppressive drugs do, however, bind in the active site of isomerase activity; see: Schreiber, S. L.; Crabtree, G. R. *Immunol. Today* **1992**, *13*, 136. It is interesting to speculate why these enzymes apparently perform two unrelated tasks by utilizing the same active site.

(13) Other postulated roles of the PPIases *in vivo* include: (a) Acting as chaperones, especially for escorting rhodopsin from the ER through the secretory pathway to its cellular target, see: Baker, E. K.; Colley, N. J.; Zuker, C. S. *EMBO J.* **1994**, *13*, 4886. (b) Effectors of Xaa-Pro bonds which may act as “molecular switches” to trigger actions such as voltage-gated ion channel opening; see: Suchyna, T. M.; Xu, L. X.; Gao, F.; Fournier, C. R.; Nicholoso, B. J. *Nature* **1993**, *365*, 847. (c) Modulation of calcium release by interaction with calcium release channels; see: Jayaraman, T.; Brillantes, A.-M.; Timmerman, A. P.; Fleischer, S.; Erdjument-Bromage, H.; Tempst, P.; Marks, A. R. *J. Biol. Chem.* **1992**, *267*, 9474. (d) Helping with protein degradation by catalyzing unfolding and prevention of partially unfolded proteins from precipitation, see: Andres, C. J.; Macdonald, T. L.; Ocaín, T. D.; Longhi, D. J. *Org. Chem.* **1993**, *58*, 6609. (e) Functioning as an auxiliary enzyme in HIV-1 protease-mediated reactions, see: Vance, J. E.; LeBlanc, D. A.; Wingfield, P.; London, R. E. *J. Biol. Chem.* **1997**, *272*, 15603.

(14) In his original reports, Karplus termed this interaction “autocatalysis” because the hydrogen bond donor was attached to the proline system either covalently or noncovalently, such as in an enzyme–substrate complex. However, this terminology may cause confusion because it is commonly used in the organic synthesis literature to mean catalysis of a reaction by its product. We therefore term this interaction intramolecular catalysis, as was proposed by Matthews.<sup>15</sup>

(15) Texter, F. L.; Spencer, D. B.; Rosenstein, R.; Matthews, C. R. *Biochemistry* **1992**, *31*, 5687.

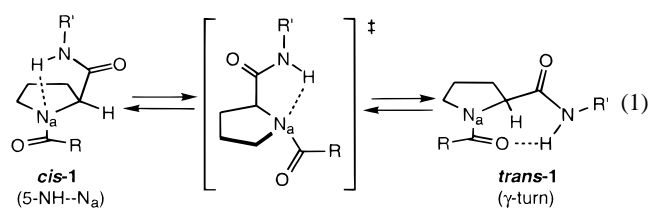
(16) For earlier discussions of [NH–N<sub>a</sub>] interactions, see: (a) Gieren, A.; Dederer, B.; Schanda, F. Z. *Naturforsch., C: Biosci.* **1980**, *35c*, 741. (b) Scarsdale, J. N.; Van Alsenoy, C.; Klimkowski, V. J.; Schäfer, L.; Momany, F. A. *J. Am. Chem. Soc.* **1983**, *105*, 3438.

(17) See for example: (a) Shoham, G.; Lipscomb, W. N.; Wieland, T. *J. Am. Chem. Soc.* **1989**, *111*, 4791. (b) Kopple, K. D.; Bhandary, K. K.; Kartha, G.; Yang, Y.-S.; Parameswaran, K. N. *J. Am. Chem. Soc.* **1986**, *108*, 4637. (c) Springer, J. P.; Cole, R. J.; Dorner, J. W.; Cox, R. H.; Richard, J. L.; Barnes, C. L.; van der Helm, D. *J. Am. Chem. Soc.* **1984**, *106*, 2388. (d) Montelione, G. T.; Arnold, E.; Meinwald, Y. C.; Stimson, E. R.; Denton, J. B.; Huang, S. G.; Clardy, J.; Scheraga, H. A. *J. Am. Chem. Soc.* **1984**, *106*, 6, 7946. (e) Karle, I. L. *J. Am. Chem. Soc.* **1979**, *101*, 181.

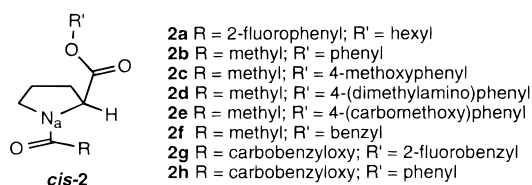
(18) Genin, M. J.; Ojala, W. H.; Gleason, W. B.; Johnson, R. L. *J. Org. Chem.* **1993**, *58*, 2334.

## Results and Discussion

**Intramolecular Catalysis in Prolyl Peptides.** At the outset, we reasoned that small peptides containing the correct structural features should show intramolecular catalysis in an organic medium that mimics the desolvated environment<sup>19</sup> of the FKBP active site, thus permitting clear-cut documentation of the 5-NH- $N_a$  H-bond unobstructed by other effects. We chose to compare activation barriers for two sterically similar prolines in organic and in aqueous/organic solution; one proline contains the catalytic NH general acid in the side chain, the other not, while both side chains are nearly isosteric. Amides **1** and esters **2** fulfill these requirements.<sup>20</sup> An  $A_{1,3}$ -like strain between the carboxamide side chain and the R substituent in *cis* prolines (*cis*-**1**) can influence their conformations;<sup>21</sup> to mitigate  $A_{1,3}$ -strain, the *cis* proline may place its side chain pseudoaxially, which would facilitate formation of the 5-NH- $N_a$  H-bond, with the carbonyl oxygen of the amide side chain oriented *exo* to the proline ring.<sup>22</sup> In nonpolar solution, we expect the *cis* form of amides **1** to contain a 5-NH- $N_a$  H-bond between the side chain and the prolyl  $N_a$ ; *this interaction should be strengthened in the transition state for cis-to-trans amide isomerization as  $N_a$  becomes more basic* (eq 1).<sup>6a</sup> The more abundant *trans* form predominantly consists of a  $\gamma$ -turn in organic solvents (*trans*-**1**).<sup>23</sup>



- 1a** R = 2-fluorophenyl; R' = hexyl  
**1b** R = methyl; R' = phenyl  
**1c** R = methyl; R' = 4-methoxyphenyl  
**1d** R = methyl; R' = 4-(dimethylamino)phenyl  
**1e** R = methyl; R' = 4-(carbomethoxy)phenyl  
**1f** R = methyl; R' = benzyl  
**1g** R = carbobenzyloxy; R' = 2-fluorobenzyl  
**1h** R = carbobenzyloxy; R' = phenyl  
**1i** R = carbobenzyloxy; R' = 4-nitrophenyl  
**1j** R = carbobenzyloxy; R' = 4-methoxyphenyl  
**1k** R = methyl; R' = 3-fluorobenzyl



We initially expected that in aqueous/organic solution intramolecular catalysis would be eliminated by competition from

(19) Liang, G.-B.; Rito, C. J.; Gellman, S. H. *J. Am. Chem. Soc.* **1992**, *114*, 4440.

(20) Many proline derivatives show poor *cis*-*trans* ratios in nonpolar solvents and/or have unresolved *cis*-*trans* rotameric signals. Our test substrates were chosen in part because sufficient *cis* form could be detected with baseline resolution to facilitate NMR analysis.

(21) Zhang, R.; Brownwell, F.; Madalengoitia, J. S. *J. Am. Chem. Soc.* **1998**, *120*, 3894.

(22) We define the carbonyl as *exo* when it is pointed away from the proline ring, whereas *endo* indicates that the carbonyl oxygen is directly over top of the ring. The *exo* carbonyl and pseudoaxially positioned side chain are clearly evident in the crystal structure of a cyclic peptide.<sup>17b</sup>

(23) It is generally accepted that the  $\gamma$ -turn is the predominate form present in organic solvents; see: (a) Madison, V.; Kopple, K. D. *J. Am. Chem. Soc.* **1980**, *102*, 4855. (b) Higashijima, T.; Tasumi, M.; Miyazawa, T. *Biopolymers* **1977**, *16*, 1259. It is unclear how much of the *trans* form is in this conformation, as opposed to a nonintramolecularly H-bonded conformation; see: (c) Liang, G.-B.; Rito, C. J.; Gellman, S. H. *Biopolymers* **1992**, *32*, 293.

the strongly H-bond-accepting solvent molecules, so intramolecular catalysis (IC) was defined as  $\Delta(\Delta G^\ddagger)$  in the change from aqueous solution to an organic solvent for model amides, subtracted by the analogous  $\Delta(\Delta G^\ddagger)$  for model esters (eq 2).<sup>7</sup> However, there are alternative ways of defining intramolecular catalysis, and one equation may not always be the most suitable for every situation. For example, if the entropy of activation ( $\Delta S^\ddagger$ ) for amide isomerization is negligible, as precedent suggests<sup>24</sup> and our results confirm (*vide infra*), intramolecular catalysis quantities defined in terms of either  $\Delta G^\ddagger$  or  $\Delta H^\ddagger$  would be similar and eqs 2 and 3 can be used interchangeably. Thus, we can compare the thermodynamically important quantity  $\Delta H^\ddagger$  in various systems without the errors commonly attendant with its measurement.<sup>25</sup> Additionally, eqs 2 and 3 presuppose that intramolecular catalysis will always be completely washed out in an aqueous environment, an assumption that we have found is not always valid (*vide infra*); nevertheless, eq 2 represents a safe *lower* limit on intramolecular catalysis. However, for isosteric substrates, there is no reason to believe that the simpler eqs 4 and 5 would not serve just as well, and can expand the range of model systems amenable to investigation due to often unfavorable separation of NMR resonances in aqueous/organic solution. The kinetics of amide isomerization in this study were measured by the highly reliable techniques of <sup>1</sup>H or <sup>19</sup>F saturation transfer (ST) NMR.<sup>26</sup>

**Intramolecular catalysis in terms of  $\Delta G^\ddagger$**  (with aqueous correction):

$$IC = [\Delta G^\ddagger_{\text{amide(aqueous)}} - \Delta G^\ddagger_{\text{amide(organic)}}] - [\Delta G^\ddagger_{\text{ester(aqueous)}} - \Delta G^\ddagger_{\text{ester(organic)}}] \quad (2)$$

**Intramolecular catalysis in terms of  $\Delta H^\ddagger$**  (with aqueous correction):

$$IC = [\Delta H^\ddagger_{\text{amide(aqueous)}} - \Delta H^\ddagger_{\text{amide(organic)}}] - [\Delta H^\ddagger_{\text{ester(aqueous)}} - \Delta H^\ddagger_{\text{ester(organic)}}] \quad (3)$$

**Intramolecular catalysis in terms of  $\Delta G^\ddagger$ :**

$$IC = [\Delta G^\ddagger_{\text{ester(organic)}} - \Delta G^\ddagger_{\text{amide(organic)}}] \quad (4)$$

**Intramolecular catalysis in terms of  $\Delta H^\ddagger$ :**

$$IC = [\Delta H^\ddagger_{\text{ester(organic)}} - \Delta H^\ddagger_{\text{amide(organic)}}] \quad (5)$$

We began our study by obtaining kinetic data for the *cis*-*trans* isomerization of prolinamide **1a** and control ester **2a** by <sup>19</sup>F saturation transfer at various temperatures. Figure 2 shows the results of a typical ST experiment on **1a**, and Figure 3 contains the Eyring plots produced from both substrates in organic and aqueous/organic solutions.<sup>27</sup> The results of the kinetic and thermodynamic analyses are collected in Table 1. In 60% MeOH/D<sub>2</sub>O,<sup>28</sup> the barriers to amide isomerization ( $\Delta G^\ddagger$ )

(24) (a) Eberhardt, E. S.; Loh, S. N.; Hinck, A. P.; Raines, R. T. *J. Am. Chem. Soc.* **1992**, *114*, 5437. (b) Drakenberg, T.; Dahlqvist, K.-I.; Forsen, S. *J. Phys. Chem.* **1972**, *76*, 2178.

(25) It is generally more accurate to determine  $\Delta G^\ddagger$  at a single temperature than to measure  $\Delta H^\ddagger$  by Eyring analysis over a limited temperature range; see: Martin, M. L.; Mabon, F.; Trierweiler, M. *J. Phys. Chem.* **1981**, *85*, 76.

(26) For applications of ST to amide isomerization, see: (a) Perrin, C. L.; Thoburn, J. D.; Kresge, J. *J. Am. Chem. Soc.* **1992**, *114*, 8800. We have used <sup>19</sup>F ST NMR to take advantage of the broad chemical shift range and generally favorable peak separations of the <sup>19</sup>F nucleus; see: (b) Cox, C.; Ferraris, D.; Murthy, N. N.; Lectka, T. *J. Am. Chem. Soc.* **1996**, *118*, 5332.

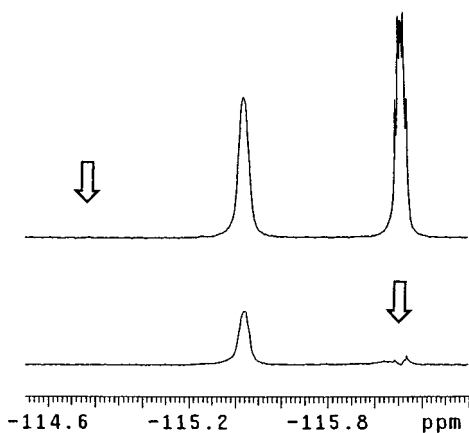


**Figure 2.** Result of  $^{19}\text{F}$  saturation transfer experiment on proline **1a**. Arrows represent the location of homonuclear decoupling.

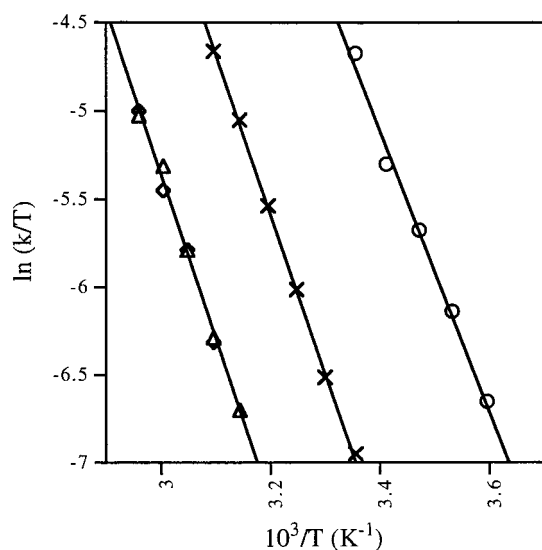


**Figure 3.** Eyring plots of **1a** in  $\text{CDCl}_3$  (O) and 60%  $\text{MeOH}/\text{D}_2\text{O}$  ( $\Delta$ ) and **2a** in  $\text{CDCl}_3$  (X) and 60%  $\text{MeOH}/\text{D}_2\text{O}$  ( $\diamond$ ).

of amide **1a** and isosteric ester **2a** were found to be identical, as expected. The equilibrium constants ( $K = [\text{trans}]/[\text{cis}]$ ) were also roughly equivalent.<sup>29</sup> In  $\text{CDCl}_3$ , however,  $\Delta G^\ddagger$  in amide **1a** dropped by 2.4 kcal/mol for *trans-to-cis* isomerization and by 3.6 kcal/mol for *cis-to-trans*, whereas in ester **2a** the respective barrier lowerings were both 1.0 kcal/mol (in line with a simple solvent effect).<sup>24</sup> Employing eq 2 thus provides a difference of 1.4 (*trans-to-cis*) and 2.6 kcal/mol (*cis-to-trans*)

(27) ST measurements on these substrates were made at 15 mM in the solvent of choice. We found the degree of intramolecular catalysis to be fairly insensitive to concentration; however, we always use equal concentration of substrates whenever direct comparisons are made. See the Experimental Section for details of the NMR experiments, calculation of rate constants, and formation of Eyring plots. For a discussion of activation parameters, see: Carpenter, B. *Determination of Organic Reaction Mechanisms*; John Wiley: New York, 1984; p 123.

(28) A mixed solvent system ( $\text{D}_2\text{O}/\text{MeOH}$ ) was necessary due to lack of solubility in pure water; in general we find that the barriers to rotation of water soluble amides in pure  $\text{D}_2\text{O}$  are not greatly different than those in  $\text{MeOH}/\text{D}_2\text{O}$  mixtures.

(29) An equilibrium constant  $K$  greater than 1 indicates that the energy of the *trans* conformation is lower than that of the *cis* form. The ester controls have a smaller  $K$  in organic solvents than the corresponding amides, due largely to the absence of the stable  $\gamma$ -turn that is present in the amides; thus, we find different values for  $\Delta G^\ddagger$  of *cis-to-trans* and of *trans-to-cis* isomerization. The former values are more significant in terms of importance in enzymatic catalysis, whereas the latter values are the ones directly measured by ST experiments (and are the ones reported throughout the paper, unless otherwise noted). The *cis-to-trans* value is obtained simply from  $K = k_{\text{trans-to-cis}}/k_{\text{cis-to-trans}}$  by plugging in the value of  $K$ .

**Table 1.** Activation Parameters and IC Values for Proline **1a** and Control Ester **2a**<sup>a</sup>

proline	solvent	$\Delta G^\ddagger$ <sup>b</sup>	$\Delta G^\ddagger$ <sup>c</sup>	$\Delta H^\ddagger$ <sup>d</sup>	$\Delta S^\ddagger$ <sup>e</sup>	$K^f$	IC <sup>g</sup>
<b>1a</b>	60% $\text{MeOH}/\text{D}_2\text{O}$	19.2	19.1	18.5	-2.4	1.2	
<b>1a</b>	$\text{CDCl}_3$	16.8	15.5	16.0	-3.0	9.8	1.4/2.6
<b>2a</b>	60% $\text{MeOH}/\text{D}_2\text{O}$	19.2	18.7	18.6	-2.2	2.2	
<b>2a</b>	$\text{CDCl}_3$	18.2	17.7	17.9	-1.1	2.5	

<sup>a</sup> Kinetics measured by  $^{19}\text{F}$  ST NMR, 15 mg/mL. See Experimental Section for details. <sup>b</sup> *Trans-cis*,  $\pm 0.2$  kcal/mol, 25 °C. <sup>c</sup> *Cis-trans*,  $\pm 0.2$  kcal/mol, 25 °C. <sup>d</sup> *Trans-cis*,  $\pm 0.3$  kcal/mol. <sup>e</sup> *Trans-cis*,  $\pm 4$  cal/(mol K). <sup>f</sup>  $K = [\text{trans}]/[\text{cis}]$ . <sup>g</sup> IC = intramolecular catalysis in kcal/mol via eq 2; first number is *trans-cis*, second is *cis-trans*.

**Table 2.** Electronic Effects on  $\Delta G^\ddagger$ <sup>a</sup>

proline	$\Delta G^\ddagger$ <sup>b</sup>	$\Delta G^\ddagger$ <sup>c</sup>	$K^d$
<b>1b</b>	16.8	15.0	25.0
<b>2b</b>	18.7	17.8	4.7
<b>1c</b>	17.0	15.3	21.1
<b>2c</b>	18.8	17.8	4.8
<b>1d</b>	17.1	15.6	14.0
<b>2d</b>	18.8	17.8	4.8
<b>1e</b>	16.5	14.2	65.1
<b>2e</b>	18.6	17.5	5.6

<sup>a</sup> Measured by  $^1\text{H}$  ST NMR, 6 mg/mL in  $\text{CD}_2\text{Cl}_2$ , 25 °C. <sup>b</sup> *Trans-cis*,  $\pm 0.2$  kcal/mol. <sup>c</sup> *Cis-trans*,  $\pm 0.2$  kcal/mol. <sup>d</sup>  $K = [\text{trans}]/[\text{cis}]$ .

that we attribute to intramolecular catalysis from the 5-NH- $\text{N}_a$  H-bond. As expected,<sup>24</sup> negligible  $\Delta S^\ddagger$  values were found in all cases, so that values for intramolecular catalysis defined in terms of either  $\Delta H^\ddagger$  or  $\Delta G^\ddagger$  are similar at 25 °C for these simple amides.

Prolines **1b–1e** with anilide side chains of different acidities and the requisite controls **2b–2e** were also analyzed kinetically as shown in Table 2.<sup>30</sup> Amide **1b**<sup>31</sup> affords intramolecular catalysis of 2.8 kcal/mol (*cis-trans*) at 25 °C in  $\text{CD}_2\text{Cl}_2$ .<sup>32</sup> Electron-donating substituents (**1c**, *p*-OMe and **1d**, *p*-NMe<sub>2</sub>) remotely placed on the aryl group show less catalysis (2.5 and 2.2 kcal/mol, *cis-trans*), whereas a remote electron-withdrawing substituent (**1e**, *p*-COOMe) exhibits the greatest degree of catalysis (3.3 kcal/mol, *cis-trans*). This latter result represents a 260-fold rate enhancement of amide isomerization over control ester **2e**. Figure 4 shows a Hammett plot of the  $\ln(\text{relative rate of amide isomerization})$  versus  $\sigma_p$ .<sup>33</sup> A direct relationship is seen between the degree of catalysis and the strength of the H-bond donor, and the positive  $\rho$  value of 2.2 indicates that electron-withdrawing groups accelerate the reaction, as expected. This result provides kinetic evidence that intramolecular catalysis due to the 5-NH- $\text{N}_a$  H-bond is indeed responsible for the enhanced rate of amide isomerization in these prolines.

**Spectroscopic Characterization.** We examined the proposed 5-NH- $\text{N}_a$  H-bond by IR and NMR spectroscopy to characterize the interaction more fully. However, complications were expected due to the predominance of the  $\gamma$ -turn between the side chain NH and the carbonyl oxygen (*trans-1*). The top trace in Figure 5 shows the high-field region of the 500 MHz NMR spectrum of proline **1f** at 10 mM in  $\text{CD}_2\text{Cl}_2$ . The presence of the *trans* and *cis* forms in a ratio of 6:1 is apparent from the

(30) We found that the  $\Delta G^\ddagger$ 's in aqueous/organic solution were identical for **1b–1e** and **2b–2e**, and therefore eq 4 is sufficient to analyze the data.

(31) Suzuki, K.; Ikegawa, A.; Mukaiyama, T. *Bull. Chem. Soc. Jpn.* **1982**, *55*, 3277.

(32) Here we find it necessary to change from  $\text{CDCl}_3$  to  $\text{CD}_2\text{Cl}_2$  due to the extremely unfavorable *cis-trans* ratio of these prolines in the former solvent. The larger dielectric constant of  $\text{CH}_2\text{Cl}_2$  increases this ratio, but we find that in general  $\Delta G^\ddagger$  is unaffected by change between these two similar chlorocarbon solvents.

(33) For a discussion of Hammett correlations and tabulated  $\sigma_p$  values, see: March, J. *Advanced Organic Chemistry*; John Wiley: New York, 1992; pp 278–286.

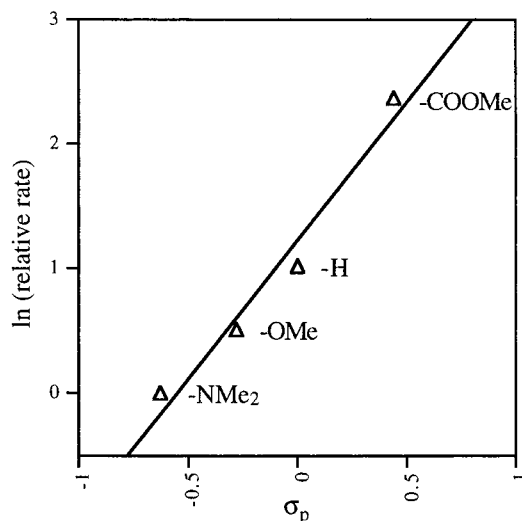


**Figure 4.** Hammett plot showing the correlation between the relative rate of amide isomerization and the electronic properties of the aryl ring.

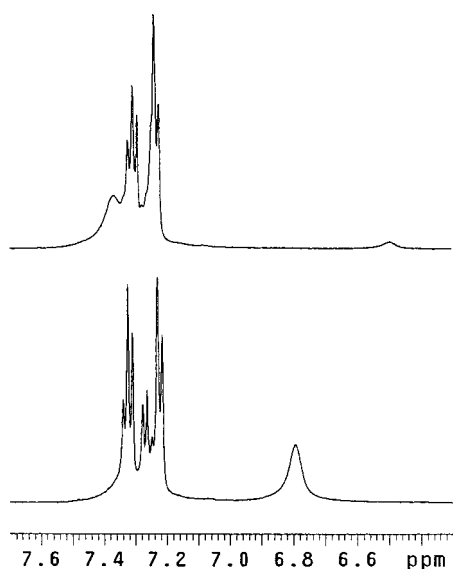
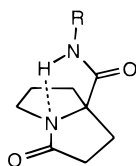


**Figure 5.** High-field region of the 500 MHz NMR spectra of proline **1f** (top) and locked amide **3a** (bottom) at 10 mM in  $\text{CD}_2\text{Cl}_2$ .

two NH resonances at 7.4 and 6.5 ppm. The top trace in Figure 6 shows the H-bonding region of the IR spectrum under the same conditions. The broad stretch centered at  $3305\text{ cm}^{-1}$  is assigned to the  $\gamma$ -turn, and the sharper stretch at  $3430\text{ cm}^{-1}$  is provisionally assigned to the 5-NH- $\text{-N}_a$  H-bond and that portion of the trans form that is not intramolecularly H-bonded.<sup>34</sup>



- 3a** R = benzyl  
**3b** R = 4-(dimethylamino)phenyl  
**3c** R = 4-methoxyphenyl  
**3d** R = 4-bromophenyl  
**3e** R = 4-(carbomethoxy)phenyl  
**3f** R = 4-nitrophenyl

For further support of the 5-NH- $\text{-N}_a$  H-bond, we desired a model system free of complications from the trans form. To this end, we synthesized proline peptidomimetics **3** which are "locked" in the cis form. Our view was that **3** should faithfully model the 5-NH- $\text{-N}_a$  unit of actual cis prolines without interference from the trans isomer; for example, the side chains of amides **3** in computer models are rigidly pseudoaxial, a prerequisite for the assembly of the 5-NH- $\text{-N}_a$  interaction. Our

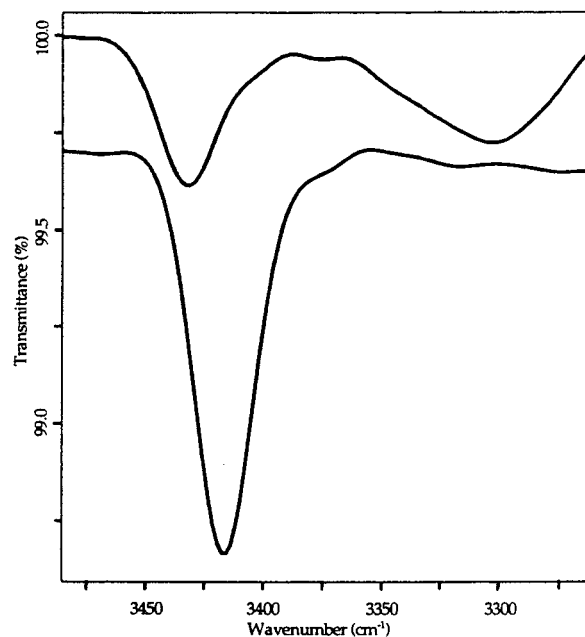
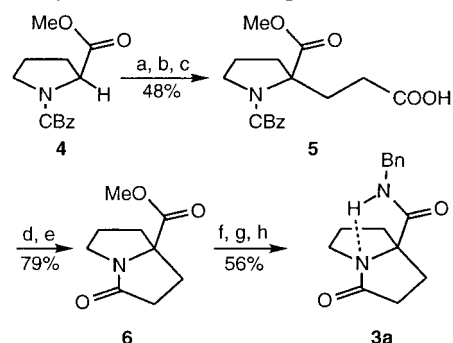


**Figure 6.** Hydrogen bonding region of the IR spectra of proline **1f** (top) and locked amide **3a** (bottom) at 10 mM in  $\text{CH}_2\text{Cl}_2$ .

#### Scheme 2. Synthesis of Locked Peptidomimetic **3a**



- a) LHMDS, allyl bromide; b) disiamylborane;  $\text{H}_2\text{O}_2$ , NaOH; c) Jones oxidation; d)  $\text{H}_2$ , Pd/C; e) EDCI; f)  $\text{Ti}(\text{O-}i\text{Pr})_4$ , BnOH; g)  $\text{H}_2$ , Pd/C; h) EDCI, BnNH<sub>2</sub>

synthesis of locked amide **3a** began with CBz-proline methyl ester **4**, which was alkylated with allyl bromide after treatment with lithium bis(trimethylsilyl)amide in THF (Scheme 2). Hydroboration with disiamylborane and oxidation with hydrogen peroxide afforded an intermediate alcohol that was subjected to Jones oxidation to afford carboxylic acid **5**. Removal of the CBz protecting group followed by EDCI-promoted<sup>5</sup> cyclization provided **6** in 79% yield from **5**. Titanium-promoted transesterification followed by benzyl ester hydrogenolysis and amidation of the intermediate acid with EDCI provided locked amide **3a** (8 steps and 21% overall yield from **4**).

The bottom traces in Figures 5 and 6 show the NMR and IR spectra of **3a** under conditions identical to those used for proline **1f**. In the  $^1\text{H}$  NMR spectrum there is a single NH resonance at 6.8 ppm, and in the IR spectrum only one NH stretch is present at  $3419\text{ cm}^{-1}$ ; this evidence is consistent with a single

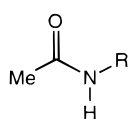
(34) This stretch has been identified in previous work as the overlapping NH stretches of both the minor cis form and also a fraction of the trans form that is not involved in a  $\gamma$ -turn (in the previous work, however, the cis form was considered to be totally non H-bonded).<sup>23c</sup> The data we have assembled herein are consistent with the belief that the stretch at higher wavenumber is due predominately to the 5-NH- $\text{-N}_a$  H-bond. Previous reports have noted that the intensity ratio of the two NH stretches is independent of concentration over a limited range in  $\text{CHCl}_3$  and  $\text{CCl}_4$ ,<sup>23b</sup> consistent with an intramolecular bond.

**Table 3.** IR Data for Locked Amides **3** and Control Amides **7**<sup>a</sup>

substrate	$\nu(\text{NH} - \text{N}_a)$	$\nu(\text{control})$	$\Delta\nu^b$	$\nu_{\text{C=O}}^c$
<b>3b</b>	3392	3432	-40	1677
<b>3c</b>	3390	3433	-43	1682
<b>3d</b>	3385	3430	-45	1690
<b>3e</b>	3381	3427	-46	1694
<b>3f</b>	3376	3426	-50	1698

<sup>a</sup> Solutions were 10 mM in  $\text{CH}_2\text{Cl}_2$ , all values in  $\text{cm}^{-1}$ . <sup>b</sup> Shift of the NH- $\text{N}_a$  bond in **3** relative to control **7**. <sup>c</sup> Stretching frequency of the endocyclic amide carbonyl.

conformation containing the 5-NH- $\text{N}_a$  H-bond. Several pieces of evidence support these assignments in locked amide **3a**: (1) The chemical shift of the NH resonance in the NMR spectrum of **3a** is independent of concentration below 15 mM, consistent with an intramolecular H-bond. Above 25 mM this peak begins to shift downfield with the onset of intermolecular H-bonding. (2) IR spectra confirm that below 15 mM only one stretch exists in the H-bonding region of **3a** (at  $3419\text{ cm}^{-1}$ ); however, at higher concentrations a broad stretch centered at  $3320\text{ cm}^{-1}$  begins to grow in, corresponding to the onset of intermolecular H-bonding. This behavior contrasts that of **1f** during dilution studies, where the relative intensities of both H-bond stretches shown in the top trace of Figure 6 are independent of concentration over a 100 mM range (data not shown). (3) Control amide **7a**,<sup>35</sup> which cannot engage in intramolecular H-bonding, has a lone IR stretch at  $3446\text{ cm}^{-1}$  at 10 mM in  $\text{CH}_2\text{Cl}_2$ , consistent with reported values for non-hydrogen bonded amide protons.<sup>36</sup> (4) The locked geometry of **3a** precludes intramolecular H-bonding between NH and the carbonyl oxygen due to geometric constraints, and therefore the intramolecular H-bond must be between NH and the prolyl  $\text{N}_a$ . These data suggest that the 5-NH- $\text{N}_a$  H-bond is the basis for the shifts of  $-27\text{ cm}^{-1}$  in locked amide **3a** and  $-16\text{ cm}^{-1}$  in proline **1f** (relative to control amide **7a**), consistent with weak H-bonding.



**7a** R = benzyl  
**7b** R = 4-(dimethylamino)phenyl  
**7c** R = 4-methoxyphenyl  
**7d** R = 4-bromophenyl  
**7e** R = 4-(carbomethoxy)phenyl  
**7f** R = 4-nitrophenyl

We also synthesized the cis locked amides **3b–3f** with anilide side chains to examine how remote functional groups effect the 5-NH- $\text{N}_a$  H-bond. As the electron-withdrawing ability of the side chain in **3** increases from 4-(dimethylamino)phenyl to 4-nitrophenyl, the catalytic H-bond stretch steadily shifts to lower wavenumber, consistent with an increasingly stronger H-bond. This shift is expected because the more strongly the *para* substituent withdraws electron density from the ring, the more acidic the side chain NH becomes. Table 3 summarizes the data on this series of locked amides, along with the values for the NH stretch of control amides **7b–7f**. As illustrated in column 4 of the table, the difference between the NH stretches of the locked amides **3** and control amides **7** ( $\Delta\nu$ ) increases as the acidity of the side chain NH increases. For instance, the locked amide **3f** (R = 4-nitrophenyl) shows a  $\Delta\nu$  of  $-50\text{ cm}^{-1}$ , the strongest 5-NH- $\text{N}_a$  H-bond characterized in this study.

As indicated in Table 3, we also find a trend in the IR stretching frequencies of the endocyclic amide C=O. The data indicate that as the strength of the 5-NH- $\text{N}_a$  H-bond increases,

(35) Pavia, A. A.; Ung-Chhun, S. N.; Durand, J.-L. *J. Org. Chem.* **1981**, *46*, 3158.

(36) Gellman has established hydrogen bound vs non-hydrogen bound amide NH IR stretching frequencies, see: Gardner, R. R.; Liang, G.-B.; Gellman, S. H. *J. Am. Chem. Soc.* **1995**, *117*, 3280 and references therein.

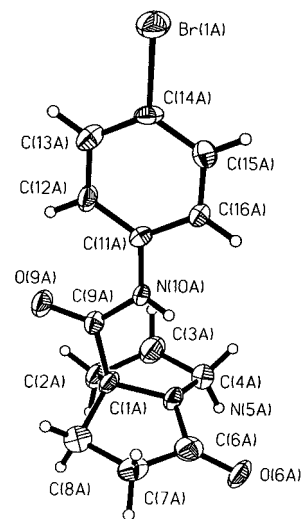


**Figure 7.** Crystal structure of **3d** (50% ellipsoids). Selected bond distances ( $\text{\AA}$ ): H(10A)–N(5A) 2.35(5); H(10A)–N(10A) 0.74(5); N(5A)–N(10A) 2.790(6). Selected bond angle (deg): N(10A)–H(10A)–N(5) 120(4).

so does the double bond character in the endocyclic amide C=O.<sup>37</sup> This correlation provides further support for a 5-NH- $\text{N}_a$  H-bond in these cis proline peptidomimetics.

**X-ray Crystallographic Studies.** Additional evidence for the 5-NH- $\text{N}_a$  H-bond comes from X-ray crystallography of **3d**,<sup>38</sup> which reveals (1) a distance from the side chain hydrogen [H(10A)] to the ring  $\text{N}_a$  [N(5A)] of  $2.35 \pm 0.05\text{ \AA}$ , (2) an N–N distance of  $2.790 \pm 0.006\text{ \AA}$ , and (3) an N(10A)–H(10A)–N(5A) bond angle of  $120 \pm 4^\circ$  (Figure 7). The position of H(10A) was refined positionally and the isotropic displacement parameter was held at 1.2 times the  $U_{\text{iso}}$  of the amide nitrogen. These bond distances and angle are such as to permit the observed 5-NH- $\text{N}_a$  interaction to be considered a weak H-bond based on the criteria of Jeffrey.<sup>39</sup> The bond of **3d** also qualifies based on sums of van der Waals radii (N and N,  $3.40\text{ \AA}$ ; N and H,  $2.70\text{ \AA}$ )<sup>40</sup> and Etter's criteria for bent NH- $\text{O}$  H-bonding in nitroaniline crystals.<sup>41</sup>

A packing diagram of **3d** is shown in Figure 8, which indicates that along with the 5-NH- $\text{N}_a$  interaction, the side chain NH also engages in a bifurcated H-bonding dimer with the side chain carbonyl of the adjacent enantiomorph. The 5-NH- $\text{N}_a$  H-bond distance in enantiomorph A is  $2.35\text{ \AA}$  (H- $\text{N}_a$  distance) and the intermolecular H-bond between this hydrogen and the adjacent proline's O(6) is  $2.334\text{ \AA}$  (N–O distance). In enantiomorph B, the corresponding distances are  $2.37$  and  $2.172\text{ \AA}$ , respectively. It is well-documented that bifurcation tends to lengthen the primary H- $\text{N}_a$  distance in H-bonding systems,<sup>42</sup> and these observations suggest that the

(37) The IR absorption discussed here, the amide I band, is primarily a C=O stretch. Work by Raines has established a direct correlation between  $\Delta G^\ddagger$  and  $\nu_{\text{C=O}}$ ; see: (a) ref 24a. Additionally, a relationship between C=O bond length and  $\nu_{\text{C=O}}$  has been found; see: (b) Bennet, A. J.; Somayajii, V.; Brown, R. S.; Santarsiero, B. D. *J. Am. Chem. Soc.* **1991**, *113*, 7563.

(38) Colorless plates of *rac*-**3d** ( $\text{C}_{14}\text{H}_{15}\text{BrN}_2\text{O}_2$ ) were grown by slow diffusion of hexane into a solution of benzene containing the amide. H[10A] was refined positionally and the asymmetric unit consists of two enantiomorphs of **3d** and one-half molecule of benzene. One antipode is depicted for simplicity. Data for **3d** collected at 173 K: monoclinic, space group  $P2_1/c$ , with  $a = 11.8158(2)\text{ \AA}$ ,  $b = 20.2329(3)\text{ \AA}$ ,  $c = 13.2733(3)\text{ \AA}$ ,  $\alpha = 90^\circ$ ,  $\beta = 104.4400(10)^\circ$ ,  $\gamma = 90^\circ$ ,  $R1 = 0.0558$ ,  $Z = 8$ ,  $\text{GOF} = 0.926$ .

(39) Jeffrey, G. A. *An Introduction to Hydrogen Bonding*; Oxford: New York, 1997; Chapter 2.

(40) Bondi, A. J. *Phys. Chem.* **1964**, *68*, 441.

(41) Panunto, T. W.; Urbánczyk-Lipkowska, Z.; Johnson, R.; Etter, M. C. *J. Am. Chem. Soc.* **1987**, *109*, 7786.

(42) Taylor, R.; Kennard, O. *Acc. Chem. Res.* **1984**, *17*, 320.

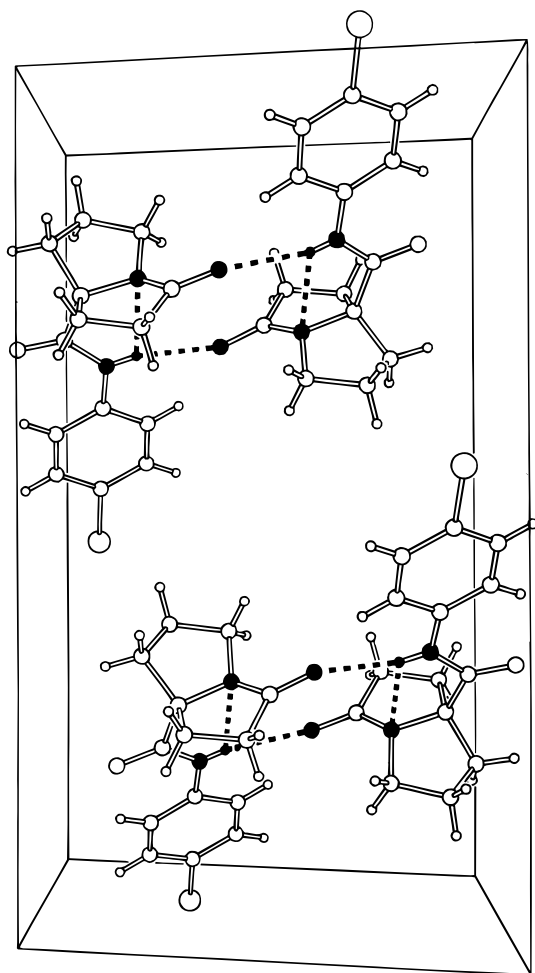
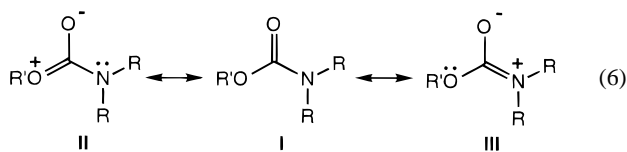


**Figure 8.** Packing diagram of **3d** showing bifurcated hydrogen bonding of the catalytic hydrogen in the solid state. The benzene molecule in the unit cell has been excluded for clarity.

5-NH- $-N_a$  H-bond we observe in the solid state may be weakened somewhat over that which we observe kinetically and spectroscopically in dilute chlorocarbon solution.

**Intramolecular Catalysis in Prolyl Carbamates.** Due to the influence of canonical form **II** in eq 6, the basicity of the nitrogen in carbamates is enhanced relative to those in corresponding amides. Previous experience with copper(II)-based Lewis acid-catalyzed amide isomerization<sup>26b</sup> led us to believe that, owing to the increased electron density at nitrogen, the degree of intramolecular catalysis for prolyl carbamates would be greater than that found in the simple amide cases discussed above. We first examined the degree of intramolecular catalysis in prolyl carbamates **1g** and **1h**<sup>43</sup> in organic solvents with respect to reference esters **2g** and **2h**, and the results are included in Table 4. The solvent for each pair was chosen so as to maximize peak separation and to facilitate NMR analysis.



The data in Table 4 in conjunction with eq 4 indicate 2.2 kcal/mol of intramolecular catalysis for prolyl carbamate **1g** with an alkyl amide side chain (entries a, b), compared to the 1.4 kcal/mol seen in the related amide **1a**. The anilide side chain

(43) Mukaiyama, T. *Tetrahedron* **1981**, 37, 4111.

**Table 4.** Activation Free Energies of Prolyl Carbamates in Organic Solvents

entry <sup>a</sup>	proline	solvent	$\Delta G^\ddagger$ <sup>b</sup>
a	<b>1g</b>	CDCl <sub>3</sub>	15.3 <sup>c</sup>
b	<b>2g</b>	CDCl <sub>3</sub>	17.5 <sup>d</sup>
c	<b>1h</b>	CD <sub>2</sub> Cl <sub>2</sub>	14.7 <sup>e</sup>
d	<b>2h</b>	CD <sub>2</sub> Cl <sub>2</sub>	17.5 <sup>d</sup>

<sup>a</sup> Entries a, b by <sup>19</sup>F ST; entries c, d by <sup>1</sup>H ST; all measurements at 10 mg/mL. <sup>b</sup> *Trans-cis*,  $\pm 0.2$  kcal/mol. <sup>c</sup>  $-10$  °C. <sup>d</sup>  $25$  °C. <sup>e</sup>  $-25$  °C.

**Table 5.** Activation Energies of Prolyl Carbamates in Aqueous Solvents

entry <sup>a</sup>	proline	solvent	$\Delta G^\ddagger$ <sup>b</sup>
a	<b>1g</b>	50% D <sub>2</sub> O/MeOH	16.4 <sup>c</sup>
b	<b>2g</b>	50% D <sub>2</sub> O/MeOH	17.5 <sup>c</sup>
c	<b>1h</b>	50% D <sub>2</sub> O/CD <sub>3</sub> CN	17.0 <sup>d</sup>
d	<b>2h</b>	50% D <sub>2</sub> O/CD <sub>3</sub> CN	17.6 <sup>d</sup>

<sup>a</sup> Entries a, b by <sup>19</sup>F ST; entries c, d by <sup>1</sup>H ST; all measurements at 10 mg/mL. <sup>b</sup> *Trans-cis*,  $\pm 0.2$  kcal/mol. <sup>c</sup>  $15$  °C. <sup>d</sup>  $25$  °C.

of carbamate **1h** provides intramolecular catalysis of 2.8 kcal/mol as calculated by eq 4 (entries c, d), whereas the analogous amide **1b** produced only 1.9 kcal/mol. These values for intramolecular catalysis in carbamates represent a lower limit due to the fact that there is residual intramolecular catalysis in aqueous/organic solution for these substrates (vide infra). Eyring analyses of substrates **1g** and **1h** in CD<sub>2</sub>Cl<sub>2</sub> were performed to determine if there was a fundamental difference in the activation parameters for isomerization in carbamates. In accord with previous reports on the isomerization of carbamates in organic solvents,<sup>25</sup> the barrier is totally enthalpic with a negligible entropy of activation. Thus, in line with our expectations, the carbamate nitrogen seemingly engages in a stronger and kinetically more significant 5-NH- $-N_a$  H-bond.

We also measured  $\Delta G^\ddagger$  for substrates **1g**, **1h** and **2g**, **2h** in aqueous/organic solution, as summarized in Table 5. The fact that **2g** and **2h** have identical  $\Delta G^\ddagger$  values in both organic and aqueous/organic solvents (cf. entries b and d in Tables 4 and 5) is consistent with our previously reported observations that  $\Delta G^\ddagger$  in carbamates is insensitive to solvent effects.<sup>44</sup> It is interesting to note that in these carbamates, as opposed to the amides, the substrates with NH side chains have lower  $\Delta G^\ddagger$  values than the isosteric controls in aqueous/organic solution. This observation is consistent with intramolecular catalysis in aqueous/organic solution that accounts for the difference of 1.1 and 0.6 kcal/mol between **1g** and **1h** and their isosteric controls **2g** and **2h**.<sup>45</sup> We then examined carbamates **1i** and **1j** in an aqueous/organic mixture to determine if the distant substituent's electronic effect could influence  $\Delta G^\ddagger$ , as was observed for prolyl amides **1b-1e** in organic solvents. However,  $\Delta G^\ddagger$  values were identical for both carbamates, indicating that the electronic differences are not large enough to exert a measurable kinetic difference in an aqueous/organic solution.

**Intramolecular Catalysis in Carbon Tetrachloride.** Although the chlorocarbon solvents used thus far are generally considered nonpolar, the relatively high dielectric of CH<sub>2</sub>Cl<sub>2</sub> ( $\epsilon = 9.1$ ) and the ability of CHCl<sub>3</sub> ( $\epsilon = 4.8$ ) to act as a hydrogen bond donor<sup>46</sup> suggest that we may not be observing the

(44) Cox, C.; Lectka, T. *J. Org. Chem.* **1998**, 63, 2426.

(45) We were not able to perform Eyring analyses on **1g** and **1h** in aqueous/organic solution because of the poor peak separation and limited temperature range available. Preliminary results on other prolyl carbamates indicate that  $\Delta G^\ddagger$  in aqueous solution is entirely enthalpic, analogous to the case of amides, in contrast to the large negative  $\Delta S^\ddagger$  we observed for acyclic tertiary carbamates.<sup>44</sup>

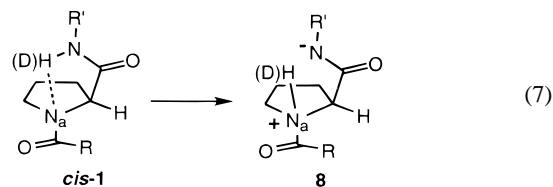
(46) Dado, G. P.; Gellman, S. H. *J. Am. Chem. Soc.* **1993**, 115, 4228.

maximum intramolecular catalysis possible. However, the poor *cis*–*trans* ratios of prolyl amides **1a**–**f** in less polar solvents such as CCl<sub>4</sub> ( $\epsilon = 2.0$ ) prohibit kinetic measurements from being performed. Prolyl carbamates, on the other hand, have more favorable *cis*–*trans* ratios in organic solvents,<sup>47</sup> and we were able to investigate carbamate **1g** and control **2g** in CCl<sub>4</sub>. These prolines, which were previously studied in CDCl<sub>3</sub> (entries a,b in Table 4), were examined in CCl<sub>4</sub>, and the  $\Delta G^\ddagger$  for isomerization was determined by ST. We found that for this system, catalysis is enhanced by 0.3 and 0.7 kcal/mol for *trans*–*to*–*cis* and *cis*–*to*–*trans* isomerization over that observed in CDCl<sub>3</sub>. This result indicates that the values reported for intramolecular catalysis of prolyl amides in CDCl<sub>3</sub> and CD<sub>2</sub>Cl<sub>2</sub> represent a lower limit to the amount of catalysis possible in nonpolar solvents.

**Thermodynamics of *Cis* Versus *Trans* Prolines.** We felt that experimental values for the thermodynamics of *cis* versus *trans* proline formation would prove helpful for future analyses of proline conformational and turn-forming properties.<sup>48</sup> To this end, we examined the temperature dependence of the *cis*–*trans* ratio in the fluorinated proline **1k** in tetrachloroethane solvent. The NH region of the IR of **1k** shows two stretches as expected; however, a cause for concern is intermolecular H-bonding, the presence of which would be hidden under the stretch for the  $\gamma$ -turn at 3310 cm<sup>-1</sup> and would significantly alter the results of our analysis. Therefore, as a control, we studied locked amide **3a** at various concentrations in tetrachloroethane and found that below 10 mM there was no evidence of intermolecular H-bonding. A van't Hoff plot of the *cis*–*trans* ratios of **1k** in 5 mM tetrachloroethane was constructed over a temperature range of 90 °C.<sup>49</sup> From the plot, we determine that the *trans* conformation is favored enthalpically by 1.7 kcal/mol, but the *cis* form is favored entropically by 60 cal/(mol K).

**Isotope Effects: Catalysis Through Hydrogen Bonding or Discrete N-Protonation?** An alternative to catalysis through intramolecular H-bonding would be intramolecular N-protonation through intermediate zwitterion **8** (eq 7). This possibility would seem to be unlikely based on (a) the *lessened degree* of intramolecular catalysis seen in polar solvents and (b) the large p*K*<sub>a</sub> difference between **1** and **8** (ca. 22–25 units). However, an amide in the transition state to isomerization (a twisted amide) would be expected to have a p*K*<sub>a</sub> closer to that of an amine; for example, Pracejus has found a p*K*<sub>a</sub> of 5.3 for the N<sub>a</sub> of a twisted amide based on a tricyclo[2.2.2]octane skeleton.<sup>50</sup> Additionally, Kirby has recently synthesized a highly twisted amide that was so labile under acidic conditions as to preclude p*K*<sub>a</sub> determination.<sup>51</sup> The transition state for amide isomerization should closely resemble Kirby's system where the lone pair is almost perfectly orthogonal to the carbonyl  $\pi$ -system, so that a p*K*<sub>a</sub> of 5.3 seems to be a safe *lower* limit for N<sub>a</sub> in the transition state for isomerization. Thus, the difference in p*K*<sub>a</sub> values of the side chain amide and N<sub>a</sub> in the transition state is reduced to a more reasonable value (<12 units). To investigate the possibility of a zwitterionic transition state, we determined the kinetic isotope effect upon replacement of the side chain amide

proton in **1a** by deuterium. For identical concentrations of **1a** and deuterated-**1a** in CDCl<sub>3</sub> at 15 °C,  $k_H/k_D = 1.00$ . The absence of an isotope effect in this system supports the H-bonding mechanism rather than discrete proton transfer to N<sub>a</sub>.



## Conclusions

We have obtained evidence, both kinetic and spectroscopic, for the existence of a 5-NH–N<sub>a</sub> H-bond that is capable of catalyzing amide isomerization by up to 260-fold in model prolyl peptides. Support for the intramolecular catalysis mechanism came from several experiments: (1) the amount of intramolecular catalysis corresponds to the acidity of the side chain NH, as evidenced by the Hammett correlation between the relative rate of amide isomerization and  $\sigma_p$  values; (2) extensive IR characterization clearly establishes the existence of an intramolecular 5-NH–N<sub>a</sub> H-bond in *cis* proline peptidomimetics and also that the strength of this bond corresponds to the acidity of the proton donor; (3) X-ray crystallographic proof of a 5-NH–N<sub>a</sub> H-bond in a *cis* proline peptidomimetic was obtained, as well as evidence that the H-bond observed in the solid state may be weakened over that present in dilute chlorocarbon solutions; (4) catalysis of amide isomerization is enhanced in prolyl carbamates relative to the analogous amides, supporting previous evidence that the carbamate nitrogen is a better H-bond acceptor than the amide nitrogen; and (5) deuterium isotope effect studies indicate that intramolecular catalysis arises from H-bonding and not from discrete N-protonation of the amide in the transition state. In addition to these results, we also discussed evidence that the degree of intramolecular catalysis observed in chlorocarbon solvents such as CHCl<sub>3</sub> and CH<sub>2</sub>Cl<sub>2</sub> is less than that in a more nonpolar solvent such as CCl<sub>4</sub>, and that a significant amount of intramolecular catalysis takes place in prolyl carbamates in aqueous solution.

We have thus verified experimentally the theoretical prediction by Karplus that intramolecular catalysis may be responsible for a significant fraction of the 6.2 kcal/mol by which the FKBP rotamase enzyme reduces  $\Delta G^\ddagger$  for *cis*–*trans* isomerization of prolyl peptides.<sup>6b</sup> These findings also support the conclusion that a 5-NH–N<sub>a</sub> hydrogen bond, prevalent in protein and natural product crystal structures, may also be involved in the intramolecular catalysis of protein folding as predicted by Matthews.<sup>15</sup> Our future work will focus on studies of the 5-NH–N<sub>a</sub> hydrogen bond in the active site of the FKBP rotamase enzyme, as well as providing experimental support for the hypothesis that a charged donor can supply the catalytic hydrogen bond required for intramolecular catalysis, as is predicted for the Arg residue in the active site of cyclophilin.

## Experimental Section

**General.** Reactions were carried out in oven- or flame-dried glassware under nitrogen, unless otherwise specified. All reagents used are commercially available from Aldrich or Sigma. Solvents were reagent grade and purified by standard techniques. EDCI is an abbreviation for 1-(3-dimethylaminopropyl)-3-ethylcarbodiimide hydrochloride, a water-soluble carbodiimide used for peptide coupling. Reactions were magnetically stirred and monitored by thin-layer chromatography on Macherey-Nagel 0.25 mm precoated plastic silica gel plates (Alltech). Flash chromatography was performed with EM

(47) The more favorable *cis*–*trans* ratio is likely due to the decreased importance of the  $\gamma$ -turn as a result of the weaker H-bond accepting ability of the carbamate carbonyl. A theoretical study has investigated the H-bond accepting properties of carbamates, see: Bandekar, J.; Okuzumi, Y. *THEOCHEM* **1993**, *281*, 113.

(48) Gellman has recently performed a somewhat similar analysis where he differentiated between the thermodynamics of  $\beta$ -turn and  $\gamma$ -turn conformations in a proline dipeptide; see ref 19.

(49) The line obtained from the van't Hoff analysis had the form  $y = 860.8x - 6.062$  with  $R^2 = 0.986$ . See the Supporting Information for the plot.

(50) Pracejus, H. *Chem. Ber.* **1959**, *92*, 988.

(51) Kirby, A. J.; Komarov, I. V.; Wothers, P. D.; Feeder, N. *Angew. Chem., Int. Ed. Engl.* **1998**, *37*, 785.

Science silica gel 60 (particle size 0.040–0.063 mm). Yields reported are for isolated, spectroscopically pure compounds unless otherwise indicated. No reactions were optimized for yield. NMR solvents were used as obtained, except that  $\text{CDCl}_3$  was dried over 4 Å molecular sieves and run through basic alumina immediately prior to use, and  $\text{CCl}_4$  was purified by filtration through silica gel. NMR spectra were recorded on a Varian Unity Plus 400 or 500 MHz spectrometer. Proton and carbon chemical shifts were referenced to residual solvent peaks or internal TMS, and fluorine shifts were referenced to external  $\text{CFCl}_3$ . NMR samples run in nondeuterated solvents were locked on a standard of either  $d_6$ -acetone or  $d_6$ -DMSO in a capillary pipet inserted into the NMR tube. *Cis*–*trans* ratios were determined by the cut-and-weigh method, which we find to be far superior to the computer integration method in terms of both accuracy and reproducibility (especially when dealing with compounds having very little *cis* isomer). As a result of two conformations being present in many of the reported compounds at room temperature, the  $^{13}\text{C}$  NMR spectra have many more lines than expected, and the  $^1\text{H}$  NMR spectra are often very complicated. Part of the complicated nature of the  $^1\text{H}$  spectra involves the fact that a peak may represent a fraction of one proton, and we account for this by reporting the integration as a decimal value. Solid and neat IR spectra were recorded on a Perkin-Elmer 1600 FTIR spectrometer, and solution phase IR were recorded with a  $\text{CaF}_2$  flow-cell on a Bruker IFS-55 FTIR spectrometer. High-resolution mass spectra were provided by the Mass Spectral Laboratory at the University of Illinois, and elemental analyses were provided by Atlantic Microlabs, Norcross GA.

**Saturation Transfer (ST) Experiments.**<sup>26a</sup> We followed rates of amide isomerization by applying a saturating decoupling pulse to a *trans* resonance in the  $^1\text{H}$  or  $^{19}\text{F}$  NMR spectra and measuring the transfer of saturation to the *cis* resonance, as well as the associated apparent spin–lattice relaxation rate. For example, the minimum power needed to saturate fully the *trans*  $^{19}\text{F}$  resonance in proline **1a** was applied, and the height of the *cis*  $^{19}\text{F}$  peak was used to determine the intensity,  $I_1$  (see Figure 2). Peak heights were found to be in fairly close agreement with those from the alternative integration method, which was used to confirm the reliability of the results. A preacquisition delay of at least  $7T_1$  was employed to allow for complete equilibration before the  $90^\circ$  observation pulse was applied.

We determined the initial intensity of the *cis* resonance,  $I_0$ , by measuring the peak height with off-resonance decoupling a distance of  $|\delta_{\text{cis}} - \delta_{\text{trans}}|$  on the opposite side of the *cis* resonance to negate any effects due to overlap of the decoupler's frequency bandwidth. The apparent spin–lattice relaxation time,  $T_1$ , of the *cis* peak was then measured by the inversion–recovery method while the *trans* site was under irradiation. Homonuclear decoupling was applied during the preacquisition delay, and during the  $\tau$  delay of the  $T_1$  measurement, but was switched off during acquisition. Apparent  $T_1$  values were obtained from manual plots of the data from the inversion–recovery experiment. This method supplies results in very good agreement with those computed by the NMR software, unless the baseline is uneven, as is the case when we are near the fast-exchange limit of detection. In that case, we assume that our manual method is more accurate because of the correction that can easily be applied for the uneven baseline by visual inspection; this assumption is validated by the excellent reproducibility we find in our manual methods versus the nonreproducible computer-generated ones.

The rate constant for isomerization,  $k$ , was then determined by eqs 8 and 9:

$$k = \% \Delta / T_1 \quad (8)$$

$$\% \Delta = (I_0 - I_1) / I_0 \quad (9)$$

Once the rate constants were determined, the free energies of activation ( $\Delta G^\ddagger$ ) for the rotational process were readily available from the Eyring equation, and  $\Delta H^\ddagger$  and  $\Delta S^\ddagger$  were available from a standard Eyring plot. All samples were allowed to equilibrate at least 15 min after probe temperature changes, and the actual probe temperature was determined by peak separation of an ethylene glycol or methanol sample. Probe temperature fluctuations during the acquisition of data were  $\leq 0.1^\circ\text{C}$ .

The number of scans necessary for each sample was determined by the signal-to-noise ratio, but was usually between 16 and 32. The reliability of our rate measurements was determined by performing the experiments in triplicate under identical conditions, which led to reproducibility of at least  $\pm 0.1$  kcal/mol for individual  $\Delta G^\ddagger$  measurements. Ranges of  $\pm 0.2$  kcal/mol are reported in the tables to allow for systematic errors. However, since we are interested only in  $\Delta(\Delta G^\ddagger)$ , the absolute values are not important, and we assume that any systematic errors mostly cancel.

**$^{19}\text{F}$  Saturation Transfer.** The most important precondition for the ST experiment is that the *cis* and *trans* resonances of the amide be well separated, so that selective irradiation can take place. In the  $^1\text{H}$  NMR spectra of many substituted prolines, this situation is not the case. Other (potentially) NMR active nuclei within the prolines pose problems of sensitivity and experimental difficulty. Especially appealing, however, is the abundance and sensitivity of the  $^{19}\text{F}$  nucleus.<sup>52</sup> Moreover, it is well-known that  $^{19}\text{F}$  spectra are very sensitive to small changes in chemical environment as a result of the large spectral range,<sup>53</sup> and fluorine atoms can be placed at remote, noninterfering positions within our prolines. ST experiments based on  $^{19}\text{F}$  have been used previously to determine the kinetics of proline isomerization in peptides.<sup>13e,54</sup>

**Eyring Plots.** Eyring plots were created by careful measurement of the rate constants of isomerization for the same sample at a minimum of five temperatures over a range of at least  $20^\circ\text{C}$ . The number of points obtained was determined by the range over which the ST method provided meaningful results; at the high-temperature limit, the *cis* resonance is completely saturated and sinks into the baseline, and at the low-temperature limit there is no difference in the initial and final height of the peak. We created the plots by graphing  $\ln(k/T)$  vs  $10^3/T$  ( $\text{K}^{-1}$ ) and standard equations were solved to determine  $\Delta H^\ddagger$  and  $\Delta S^\ddagger$ .<sup>27</sup> The correlation of the line was usually 0.99 or better. The listed errors in  $\Delta H^\ddagger$  were determined from least-squares analysis of the Eyring plot. Questions have been raised about the reliability of  $\Delta S^\ddagger$  values from data obtained over a limited temperature range.<sup>25</sup> We conservatively report our error in  $\Delta S^\ddagger$  as  $\pm 4$  cal/(mol K), even though least-squares analysis of the Eyring data usually indicates  $\pm 2$  cal/(mol K). We have performed in excess of 30 Eyring analyses on amides and carbamates, and in no case (other than special ones where we now expect  $\Delta S^\ddagger$  to deviate from zero<sup>44</sup>) have we found  $\Delta S^\ddagger$  to deviate from zero by more than 3.3 cal/(mol K).

**Isotopic Exchange.** To 100 mg of **1a** was added 10 mL of  $\text{CH}_3\text{-COOD}$ , and the mixture was stirred for 1 h in a glovebox under  $\text{N}_2$ . The solvent was then removed in vacuo and the process repeated 5 times. The deuterium-enriched material in the glovebox was added to an NMR tube (that had been rinsed several times with  $\text{CH}_3\text{COOD}$  and dried under vacuum) and then dissolved in freshly distilled  $\text{CDCl}_3$ . The isotopic purity was judged  $>90\%$  by  $^1\text{H}$  NMR.

**Acknowledgment.** T.L. thanks the NIH (R29 GM54348) and the American Cancer Society for support of this work. C.C. thanks the Organic Division of the American Chemical Society for a Graduate Fellowship (sponsored by Organic Reactions, Inc.) and JHU for a Marks Fellowship. The authors thank Professor John Toscano for use of his FTIR spectrometer and Dr. Victor G. Young, Jr., director of the X-ray Crystallographic Laboratory at the University of Minnesota, for solving the structure of **3d**. We also thank Professor Alex Nickon and a referee for providing insightful comments on the manuscript.

**Supporting Information Available:** X-ray crystallographic data for **3d**, van't Hoff plot of **1k**, and synthetic details and characterization data for all new compounds (28 pages, print/PDF). See any current masthead page for ordering information and Web access instructions.

JA9815071

(52)  $^{19}\text{F}$  is a spin  $1/2$  nucleus with 100% natural abundance and is 83% as sensitive as  $^1\text{H}$ ; see: Abraham, R. J.; Fisher, J.; Loftus, P. *Introduction to NMR Spectroscopy*; Wiley: New York, 1993; Chapter 1.

(53) Sievers, R. E.; Bayer, E.; Hunziker, P. *Nature* **1969**, 223, 179.

(54) London, R. E.; Davis, D. G.; Vavrek, R. J.; Stewart, J. M.; Handschumacher, R. E. *Biochemistry* **1990**, 29, 10298.